



Contents lists available at ScienceDirect

Translational Research

journal homepage: www.elsevier.com/locate/jagp

Tumor suppressor role of RBM22 in prostate cancer acting as a dual-factor regulating alternative splicing and transcription of key oncogenic genes

Juan M. Jiménez-Vacas^{a,b,c,d,*}, Antonio J. Montero-Hidalgo^{a,b,c,d}, Enrique Gómez-Gómez^{a,c,e}, Prudencio Sáez-Martínez^{a,b,c,d}, Antonio C. Fuentes-Fayos^{a,b,c,d}, Adrià Closa^{f,g}, Teresa González-Serrano^{a,c,h}, Ana Martínez-López^{c,h}, Rafael Sánchez-Sánchez^{a,c,h}, Pedro P. López-Casasⁱ, André Sarmento-Cabral^{a,b,c,d}, David Olmosⁱ, Eduardo Eyras^{f,g,j,k}, Justo P. Castaño^{a,b,c,d}, Manuel D. Gahete^{a,b,c,d}, Raul M. Luque^{a,b,c,d,*}

^a Maimonides Institute for Biomedical Research of Córdoba (IMIBIC), Córdoba, Spain

^b Department of Cell Biology, Physiology, and Immunology, University of Córdoba, Córdoba, Spain

^c Hospital Universitario Reina Sofía (HURS), Córdoba, Spain

^d Centro de Investigación Biomédica en Red de Fisiopatología de la Obesidad y Nutrición, (CIBEROBN), Córdoba, Spain

^e Urology Service, HURS/IMIBIC, Córdoba, Spain

^f The John Curtin School of Medical Research, Australian National University, Canberra, Australia

^g EMBL Australia Partner Laboratory Network at the Australian National University, Canberra, Australia

^h Anatomical Pathology Service, HURS, Córdoba, Spain

ⁱ Prostate Cancer Clinical Research Unit, Hospital Universitario 12 de Octubre, Instituto de Investigación Sanitaria Hospital 12 de Octubre (imas12), Madrid, Spain

^j Catalan Institution for Research and Advanced Studies, Barcelona, Spain

^k Hospital del Mar Medical Research Institute (IMIM), Barcelona, Spain

ARTICLE INFO

ABSTRACT

Prostate cancer (PCa) is one of the leading causes of cancer-related deaths among men. Consequently, the identification of novel molecular targets for treatment is urgently needed to improve patients' outcomes. Our group recently reported that some elements of the cellular machinery controlling alternative-splicing might be useful as potential novel therapeutic tools against advanced PCa. However, the presence and functional role of RBM22, a key spliceosome component, in PCa remains unknown. Therefore, RBM22 levels were firstly interrogated in 3 human cohorts and 2 preclinical mouse models (TRAMP/Pbsn-Myc). Results were validated in *in silico* using 2 additional cohorts. Then, functional effects in response to RBM22 overexpression (proliferation, migration, tumorspheres/colonies formation) were tested in PCa models *in vitro* (LNCaP, 22Rv1, and PC-3 cell-lines) and *in vivo* (xenograft). High throughput methods (ie, RNA-seq, nCounter PanCancer Pathways Panel) were performed in RBM22 overexpressing cells and xenograft tumors. We found that RBM22 levels were down-regulated (mRNA and protein) in PCa samples, and were inversely associated with key clinical aggressiveness features. Consistently, a gradual reduction of RBM22 from non-tumor to poorly differentiated PCa samples was observed in transgenic models (TRAMP/Pbsn-Myc). Notably, RBM22 overexpression decreased aggressiveness features *in vitro*, and *in vivo*. These actions were associated with the splicing dysregulation of numerous genes and to the downregulation of critical upstream regulators of cell-cycle (i.e., *CDK1/CCND1/EPAS1*). Altogether, our data demonstrate that RBM22 plays a critical pathophysiological role in PCa and invites to suggest that targeting negative regulators of RBM22 expression/activity could represent a novel therapeutic strategy to tackle this disease.

Abbreviation: AR, androgen receptor; BPH, benign prostatic hyperplasia; FDR, false discovery rate; FFPE, formalin-fixed, paraffin-embedded; GS, gleason score; IHC, immunohistochemistry; IPA, ingenuity pathway analysis; MD-PCa, moderately differentiated prostate cancer; N-TAR, non-tumor adjacent region; PCa, prostate cancer; PD-PCa, poorly differentiated prostate cancer; PI3K, phosphoinositide 3-kinase; PIN, prostatic intraepithelial neoplasia; RBM22, RNA binding motif protein 22; RRM, rna recognition motif; TRAMP, transgenic adenocarcinoma of mouse prostate model

* Reprint requests: Juan M. Jiménez-Vacas and Raúl M. Luque. Maimonides Institute for Biomedical Research of Córdoba (IMIBIC), IMIBIC Building. Av. Menéndez Pidal s/n. 14004-Córdoba, Spain.

E-mail addresses: b12jivaj@uco.es (J.M. Jiménez-Vacas), raul.luque@uco.es, bc2luhur@uco.es (R.M. Luque).

Juan M. Jiménez-Vacas and Antonio J. Montero-Hidalgo contributed equally to this work and should be considered co-first authors.

<https://doi.org/10.1016/j.trsl.2022.08.016>

Received 17 June 2022; Revised 7 August 2022; Accepted 24 August 2022

At A Glance Commentary

Jimenez-Vacas JM, et al.

Background

The importance of alternative-splicing dysregulation in prostate cancer (PCa) is indisputable. However, the contribution of components of the molecular machinery controlling the splicing process remains poorly explored in PCa.

Translational Significance

Our results identified the RNA Binding-Motif 22 (RBM22) as a key splicing-factor regulating clinically relevant pathological functions with therapeutic potential in PCa. Indeed, RBM22 expression was downregulated in PCa, and its overexpression reduced tumor aggressiveness *in vitro* and *in vivo* through cell-cycle arrest in PCa-cells. Additionally, RBM22 high expressing PCa cells downregulated CDK1/ATR, and consequently are candidate for PARP-inhibition. Altogether, these findings indicate that RBM22 could represent a predictive-biomarker/therapeutic-target in PCa.

Introduction

Prostate cancer (PCa) is the commonest cancer in men and a leading cause of cancer-related death in developed countries.¹ PCa is highly heterogeneous, encompassing from slow-growing/indolent to aggressive/clinically-significant tumors, which hampers its clinical management.² In this scenario, although low aggressive localized lesions (ie Gleason score 6) are curable, the treatment of highly aggressive locally advanced PCa and metastatic PCa remains challenging.^{3,4} Indeed, despite the initial robust responses to new generation AR-signaling targeting agents (ie abiraterone, enzalutamide, apalutamide and darolutamide) and taxanes (ie docetaxel and cabazitaxel), advanced PCa eventually become resistant, then representing a lethal disease.^{4,5} In this scenario, therapeutically exploitable molecular drivers of highly aggressive PCa comprise aberrations in androgen receptor (AR), phosphoinositide 3-kinase (PI3K), and DNA repair signaling pathways, among others.^{3,6,7} Although specific subsets of patients benefit from these personalized strategies, the high biologic diversity, and the intra- and inter-patient heterogeneity of PCa hamper their long-term efficacy.^{8,9} Therefore, a more profound knowledge of highly aggressive PCa biology is required to identify new therapeutic targets to tackle this lethal disease.

In this sense, nowadays it is well-recognized that the splicing process and its regulation are highly relevant for understanding every hallmark of cancer, to the point that splicing alterations constitute another cancer hallmark.¹⁰⁻¹² Recent and increasing evidence from our group and others has documented that the machinery controlling the splicing process is often altered in different cancer types, which translates in an augmented pathological versatility (eg through generation of distinct/novel alternative splicing variants).¹³⁻¹⁸ Likewise, proteins involved in the regulation of splicing (splicing factors [SFs]) play an oncogenic role in PCa by regulating mRNA splicing as well as other mRNA-metabolism processes and might represent exploitable therapeutic targets.^{19,20} More specifically, RNA binding motif (RBM) family members have particularly become a focus of interest in PCa field, given the essential role that some of these elements play in the progression of several tumor-types, including PCa.²¹⁻²⁴ Among them, RBM22 stands out as a key member of the RBM family, since it is involved in the: (1) Activation of the spliceosome, by interacting with the U6 internal stem-loop and the pre-mRNA intron,^{25,26} and (2) Regulation of gene expression, presumably acting as a transcription factor.^{27,28} Remarkably, although RBM22 has been associated with certain tumor-types, by regulating survival, mitosis and differentiation processes pathways,²⁹ its role in PCa remains completely unknown.

Therefore, in the present study we used samples from 3 different well-characterized cohorts of PCa patients, various cellular (*in vitro*) and

preclinical (*in vivo*) models, and a wide set of functional and molecular assays to evaluate RBM22 levels and its implication in the development, progression, and aggressiveness of PCa.

Material and methods

Patients and samples

The experimental study of human PCa samples was approved by the Reina Sofia University Hospital Ethics Committee and conducted in accordance with the principles of the Declaration of Helsinki. The regional Biobank coordinated the collection, processing, management, and assignment of the biological samples used in the present study according to the standard procedures established for this purpose. Written informed consent was obtained from all patients. Three different cohorts of prostate samples were collected and analyzed:

- **Cohort 1**) formalin-fixed, paraffin-embedded (FFPE) PCa tissues (n = 84) and their non-tumor adjacent region (N-TAR; used as control tissues; n = 84), taken from radical prostatectomies from patients diagnosed with clinically localized PCa (Table I). The presence or absence of tumor was defined according to pathology review of haematoxylin/eosin-stained tissue. This cohort was used for RNA expression analysis.
- **Cohort 2**) fresh samples that were obtained by: (1) core needle biopsies from patients with significant PCa (n = 42; Table II); and (2) cystoprostatectomies from patients without PCa (n = 9; used as control tissue). The presence or absence of tumor was histologically confirmed by uro-pathologists. This cohort was also used for RNA analysis.
- **Cohort 3**) An additional set of samples was used for immunohistochemistry (IHC) analysis, which included tissue samples from benign prostatic hyperplasia (n = 11), prostatic intraepithelial neoplasia (n = 6), and PCa with GS 6 (n = 5).

The clinical parameters collected from each patient were Gleason Score (GS; analyzed by uro-pathologists following the modified 2014 ISUP criteria), T-Stage, perineural invasion, lymphovascular invasion and presence of metastases at diagnosis (determined by computed tomography and bone scan).

In addition, gene expression and clinical data from 3 additional and available *in silico* cohorts of patients (ie **Lapointe**, **TCGA** and **SU2C/PCF cohorts**) were downloaded from cBioPortal and GEO datasets.³⁰⁻³⁴

Cell lines and reagents

Cell lines derived from normal prostate epithelium (RWPE-1) and PCa (LNCaP, 22Rv1 and PC-3) were obtained from the American Type Culture Collection (ATCC; Manassas, VA, USA) and cultured in a humidified incubator with 5% CO₂ at 37°C according to ATCC recommendations, as previously described.^{13,15,16} Cell line identity was validated by

Table I
Demographic, biochemical and clinical parameters of the patients from cohort 1

Patients [n]	84
Age, years (median [IQR])	61 (57-66)
PSA levels, ng/mL (median [IQR])	5.2 (4.2-8.0)
Gleason score ≥ 7 (n (%))	76 (90.5%)
pT $\geq 3a$ (n (%))	59 (70.2%)
PI (n (%))	72 (85.7%)
VI (n (%))	8 (9.52%)
Recurrence (n (%))	35 (41.7%)
Metastasis [n (%)]	0 (0%)

PI: Perineural invasion; PSA: Prostate specific antigen; pT: Pathological primary tumor staging; VI: Vascular invasion.

Table II
Demographic, biochemical and clinical parameters of the patients from cohort 2

Patients [n]	42
Age, years (median [IQR])	75 (69–81)
PSA levels, ng/mL [median (IQR)]	62.0 (36.2–254.5)
Gleason score ≥ 7 (n (%))	42 (100%)
Metastasis (n [%])	28 (66.7%)

PSA: Prostate specific antigen; SigPCa: Significant PCa defined as Gleason score ≥ 7 .

short tandem repeats sequences (STRs) analysis. All cell lines were tested for mycoplasma by PCR, as previously reported.^{13,15,16} Dihydrotestosterone (DHT, S4757, Selleckchem, USA) was used at 10 nM.

RNA-isolation, retrotranscription and real-time quantitative PCR (qPCR)

RNA from FFPE samples, fresh tissues and cell-lines was isolated as previously reported.^{35–37} Briefly, Maxwell 16 LEVRNA FFPE Kit (Promega, Madison, USA) was used in the Maxwell MDx 16 Instrument (Promega, Madrid, Spain) to isolate RNA from FFPE samples. Additionally, AllPrep DNA/RNA/Protein Mini Kit (Qiagen) and TRIzol Reagent (Thermo Fisher Scientific, Waltham, MA, USA) were used to isolate RNA from fresh tissues and PCa cell lines, respectively. RNA was DNase-treated using RNase-Free DNase Kit (Qiagen). Total RNA concentration and purity were assessed using Nanodrop One Spectrophotometer (Thermo Fisher Scientific, Madrid, Spain). Total RNA was retrotranscribed using random hexamer primers and the cDNA First Strand Synthesis kit (Thermo Scientific). Details regarding the development and validation of the primers for real time qPCR were previously reported by our laboratory.^{35–37} Detailed information about the primers used herein (ie human *RBM22*, *ACTB* and *GAPDH* as well as mouse *Rbm22* and *Ppia*) can be found in Supplemental Table 1. A normalization factor (calculated with *ACTB* and *GAPDH* expression levels, using GeNorm 3.3³⁸) and *Ppia* expression levels were used to adjust mRNA expression levels of the human and mouse genes, respectively.

Immunohistochemistry

IHC analysis was performed on samples from cohort 1 and cohort 3. The IHC protocol followed in this study was previously described.¹³ Briefly, deparaffinized sections were incubated overnight (4°C) with the anti-RBM22 antibody (ab59157, Abcam Cambridge, UK) at 1:250 dilution, followed by incubation with an anti-rabbit horseradish peroxidase-conjugated secondary antibody (#7074; Cell Signalling). Finally, sections were developed with 3,3'-diaminobenzidine (Envision system 2-Kit Solution DAB) and contrasted with haematoxylin. Independent pathologists performed histopathologic analyses indicating low, moderate, and high intensities of nuclear staining, following a blinded protocol.

Stable transfection of RBM22

LNCAp, 22Rv1 and PC-3 cells were stably transfected as previously reported.^{15,16} Briefly, cells were transfected with 1 μ g of RBM22 plasmid (OHu02939, GenScript) using Lipofectamine-2000 (Gibco, Barcelona, Spain) following manufacturer's instructions. Moreover, cells transfected with 1 μ g of pcDNA3.1 empty plasmid were used as control (called mock from now on). Transfected cells were selected by the continuous addition of geneticin at 1% (Gibco).

Cell proliferation assay

Cell proliferation was assessed by alamar-blue assay (Bio-SOURCE International, Camarillo, CA, USA) as previously reported.^{13,15,16} In response to RBM22 overexpression in LNCAp, 22Rv1 and PC-3. Specifically, 3,000 cells

per well were seeded in 96-well plates, serum-starved overnight, and then fluorescence (540 nm excitation and 590 nm emission) was measured (after 3hour incubation with 10% resazurin) at 24, 48 and 72 hour using the FlexStation III system (Molecular Devices, Sunnyvale, CA, USA). All the data were normalized to values obtained in day 0 and represented as fold change compared to mock-transfected cells.

Cell migration assay

Cell migration was evaluated in PC-3, given its high invasiveness nature.³⁹ Specifically, 500,000 cells were seeded in 12-well plates. When confluence was reached, a scratch was made in each well, using a 100 μ L tip and complete media was replaced by no serum media. Images were taken immediately after doing the scratch and 12 hour after. Wound healing was calculated as the area observed 12 hour after the wound was made vs the area observed just after wounding.

Tumorspheres formation assay

Tumorsphere formation assay was carried out, in LNCAp and PC-3 in response to RBM22 overexpression, as previously reported.^{14,40} Briefly, 2,000 cells/well were seeded in Corning Costar 24-well ultra-low attachment plates (Merck, Madrid, Spain) with DMEM F-12 medium supplemented with 20 ng/mL EGF (Sigma-Aldrich, Madrid, Spain). The number of tumorspheres was determined after 14 days of incubation with ImageJ software.

Colony formation assay

To determine the clonogenic capacity of LNCAp and PC-3 cells in response to RBM22 overexpression, 2,000 cells were seeded into 6-well plates. Then, the medium was removed, the colonies washed with PBS and stained with crystal violet for 30 min and air-dried. The number of individual colonies and the percent of area covered with colonies by colony area were determined by ImageJ software (colony area plugin).

RNA sequencing (RNAseq) in RBM22-overexpressing PCa cells

RNA integrity of total RNA (500ng) from RBM22-overexpressing PC-3 cells (n = 3) and mock PC-3 cells (n = 3) was assessed using the Agilent 2100 Bioanalyzer. RNAseq was performed at the Genomics Core Unit of The National Centre for Cancer Research (CNIO), Madrid, Spain. Briefly, PolyA+ fraction was purified and randomly fragmented, converted to double-stranded cDNA and processed through subsequent enzymatic treatments of end-repair, dA-tailing, and ligation to adapters (NEBNext Ultra II Directional RNA Library Prep Kit for Illumina, NEB #E7760), as recommended by the kit manufacturer. Adapter-ligated library was completed by PCR with Illumina PE primers. The resulting purified cDNA libraries, with an average size of 400bp, were applied to an Illumina flow cell for cluster generation and sequenced on an Illumina instrument following manufacturer's protocols. Image analysis, per-cycle base-calling and quality score assignment were performed with Illumina HiSeq Control Software. Conversion of BCL files to FASTQ format was performed with the bcl2fastq Software (Illumina). Quantification at transcription level was developed using the Gencode transcriptome release 27 (GRCH38.p10)⁴¹ in transcripts per million (TPM) units with Salmon (v 0.7.2).⁴² Gene level quantification was obtained by transforming transcript TPMs to counts per gene using the tximport library function from Bioconductor.⁴³ Counts were transformed to log2 counts per million (logCPM) and filtered genes with mean logCPM < 0 were filtered out. Normalization was performed using TMM method from edgeR package and differentially expressed genes (DEGs) were analyzed using LIMMA package using limma-voom function adjusted using SVA package to remove batch effects.⁴⁴ DEGs were functionally analyzed using Ingenuity Pathway Analysis (IPA, QIAGEN Redwood City, CA, USA, www.qiagen.com/ingenuity) to determine disease and

function pathways, canonical pathways, and master regulators. The metrics entered were z-score and adjusted *P*-value, and default settings were used for the analysis. Pathways with z-score > 2 were considered “activated” and those with z-score < -2 were considered “inhibited”. SUPPA generateEvents was used to generate alternative splicing events defined from protein-coding transcripts and covering the annotated ORFs.^{45,46} The relative inclusion of an event was calculated as a Percent Spliced In (PSI) value with SUPPA psiPerEvent from the transcript TPM values obtained before. We applied a linear regression model to estimate the significance of the splicing changes and adjusted the *P*-value by calculating a false discovery rate (FDR). We considered significant the changes with an FDR corrected *P*-value < 0.05.

Preclinical models of PCa

Experiments with mice were carried out according to the European Regulations for Animal Care under the approval of the university/regional government research ethics committees.

For tumor growth experiments, ten-week-old male athymic BALB/cAnNRj-Foxn1nu mice (Janvier Labs, Le Genest-Saint-Isle, France) were subcutaneously grafted in both flanks with 3×10^6 viable mock-transfected ($n = 5$ mice; $n = 10$ tumors) or RBM22-stably transfected PC-3 cells ($n = 5$ mice; $n = 10$ tumors) that were resuspended in 100 mL of basement membrane extract (Trevigen, Gaithersburg, MD, USA). Tumor growth was monitored once per week for 2 months using a digital caliper. After euthanization of mice, each tumor was kept at -80°C for later RNA extraction by using TRIzol reagent (Thermo Fisher Scientific) or protein extraction using SDS-DTT buffer as previously reported.^{15,16}

Additionally, in order to determine the expression of RBM22 during PCa progression *in vivo*, we used the transgenic adenocarcinoma of mouse prostate (TRAMP) mice, heterozygous for the PB-Tag transgene, maintained in a C57BL/6 background and crossed with non-transgenic FVB mice to obtain transgenic (C57BL/6 × FVB) F1 males. TRAMP mice were sacrificed at 13, 21, and 30 weeks of age, when it has been demonstrated that these mice develop PIN, moderately differentiated PCa and poorly differentiated PCa, respectively.⁴⁷ Findings were then confirmed in a second PCa mouse model: the Hi-Myc (ARR2/Pbsn-Myc) mouse strain maintained in an FVB background which was obtained originally from NCI and backcrossed to C57BL/6 for more than 7 generations at Dr Olmos lab at CNIO to obtain pure genetic background. Hi-Myc mice were sacrificed at 4 months (No tumor), 6–8 months (predominantly PIN) and 12–15 months (predominately invasive carcinoma). PCR genotyping in both models was performed in genomic DNA extracted from the tail vein blood by PCR. TRAMP model was genotyped using the primers recommended by The Jackson Laboratory for TRAMP (Sense: TACAAGTCCAACTGGGATG; Antisense: CAGGCACTCCTTCAAGACC) and those recommended by NCI⁴⁷ to examine the transgene (sense: AAACATGATGACTACCAAGCTTGGC; antisense: ATGATAGCATCTTGTCTT AGTCTTTTCTTAATAGGG). All prostate tissues were processed and divide in specular fragments for formalin-fixation and paraffin inclusion or stored as fresh-frozen tissue at -80°C and used for gene expression and protein analysis.

nCOUNTER analysis

nCounter PanCancer Pathways Panel kit (GXA-PATH1-12; NanoString Technologies) was used and performed at the Laboratory of Genetics at UCAIB (IMIBIC) to simultaneously examine the expression of 730 genes associated with cancer (ie 606 genes representing all major cancer pathways and 124 key cancer driver genes), as previously described.⁴⁸ Briefly, the quality of all samples (RBM22-overexpressing xenograft tumors [derived from PC-3 cells; $n = 3$] and mock-overexpressing tumors [derived from PC-3 cells; $n = 3$]) was analyzed using the Agilent 2100 Bioanalyzer. Then, 100ng of RNA from all the samples were loaded in the nCounter PanCancer Pathways Panel kit and the experiment was run in the nCounter Analysis

System (NanoString Technologies), following manufacturer’s protocol. The data were analyzed using the nSolverAnalysisSoftware 3.0.22 from NanoStringTechnologies. Data were normalized using 40 genes as housekeeping genes as previously described.⁴⁸ All specific target sequences and panel details are available on the manufacturer’s webpage.

Statistical analysis

All the experiments were performed in at least 3 independent experiments ($n \geq 3$). Statistical differences between 2 variables were calculated by unpaired parametric *t*-test and nonparametric Mann Whitney U test, according to normality, assessed by Kolmogorov-Smirnov test. For differences among 3 variables, 1-Way ANOVA analysis was performed. Statistical significance was considered when $P < 0.05$. A trend for significance was indicated when *P* values ranged between >0.05 and <0.1. All the analyses were assessed using GraphPad Prism 8 (GraphPad Software, La Jolla, CA, USA).

Results

RBM22 levels are significantly decreased in PCa and inversely associate with key clinical and molecular features of aggressiveness

RBM22 mRNA levels were slightly but consistently lower in PCa tissues as compared to non-tumor prostate tissues in 2 independent cohorts of samples available in our laboratory (cohort 1 and 2; Fig 1A). Consistently, downregulation of RBM22 in PCa was also observed in 2 independent cohorts of patients available *in silico*, Lapointe and TCGA datasets^{32,33} (Fig 1B). Genetic status of RBM22 was interrogated in the TCGA dataset (primary PCa samples, PanCancer Atlas)³³ and in SU2C/PCF cohort (mCRPC samples).³⁴ Specifically, although genomic alterations of RBM22 were not common in these cohorts, RBM22 mRNA levels were associated with RBM22 copy number (Supplemental Figure 1A and 1B). On the other hand, RBM22 mRNA levels did not consistently associate with any molecular subtype or common genomic aberration of PCa (Supplemental Figure 1C and 1D). Further clinical and molecular interrogation of tumor biopsies revealed that lower RBM22 expression levels were associated with extraprostatic extension and perineural invasion capacity (Fig 1C), but not with disease free survival or overall survival in TCGA and SU2C/PCF cohorts, respectively (Supplemental Figure 2). Moreover, the expression levels of RBM22 tended to be inversely correlated with those of KLK3 and PCA3 (Fig 1D), while non-significant correlations/associations were found when analyzing Gleason Score, plasma PSA levels, age or presence of metastasis (Supplemental Figure 3A and 3B). Likewise, expression levels of RBM22 were not significantly correlated to those of AR, AR-V7 or MKI67 in our cohort of samples (Supplemental Figure 3C).

Then, RBM22 protein levels were analyzed in a set of biopsies samples which included benign prostatic hyperplasia (BPH), prostatic intraepithelial neoplasia (PIN) and PCa tissues (Fig 1E). Consistent with the previous data observed at the mRNA level, the protein levels of RBM22 were significantly lower in PCa samples as compared to non-tumor and BPH tissues (Fig 1E). Moreover, consistent also with its role as splicing and transcription factor, RBM22 staining was exclusively detected in the nucleus of the cells (Fig 1E). Interestingly, RBM22 protein levels were especially low in PCa samples with Gleason score ≥ 7 (Fig 1F). Likewise, RBM22 staining tended to be ($P = 0.082$) lower in diagnostic biopsies from patients with metastasis compared with those without metastasis (Fig 1G).

Low RBM22 levels are associated with poorly differentiated prostate cancer in the TRAMP model

The TRAMP mouse model mimics the progression of human PCa by developing PIN, moderately-differentiated prostate cancer (MD-PCa)

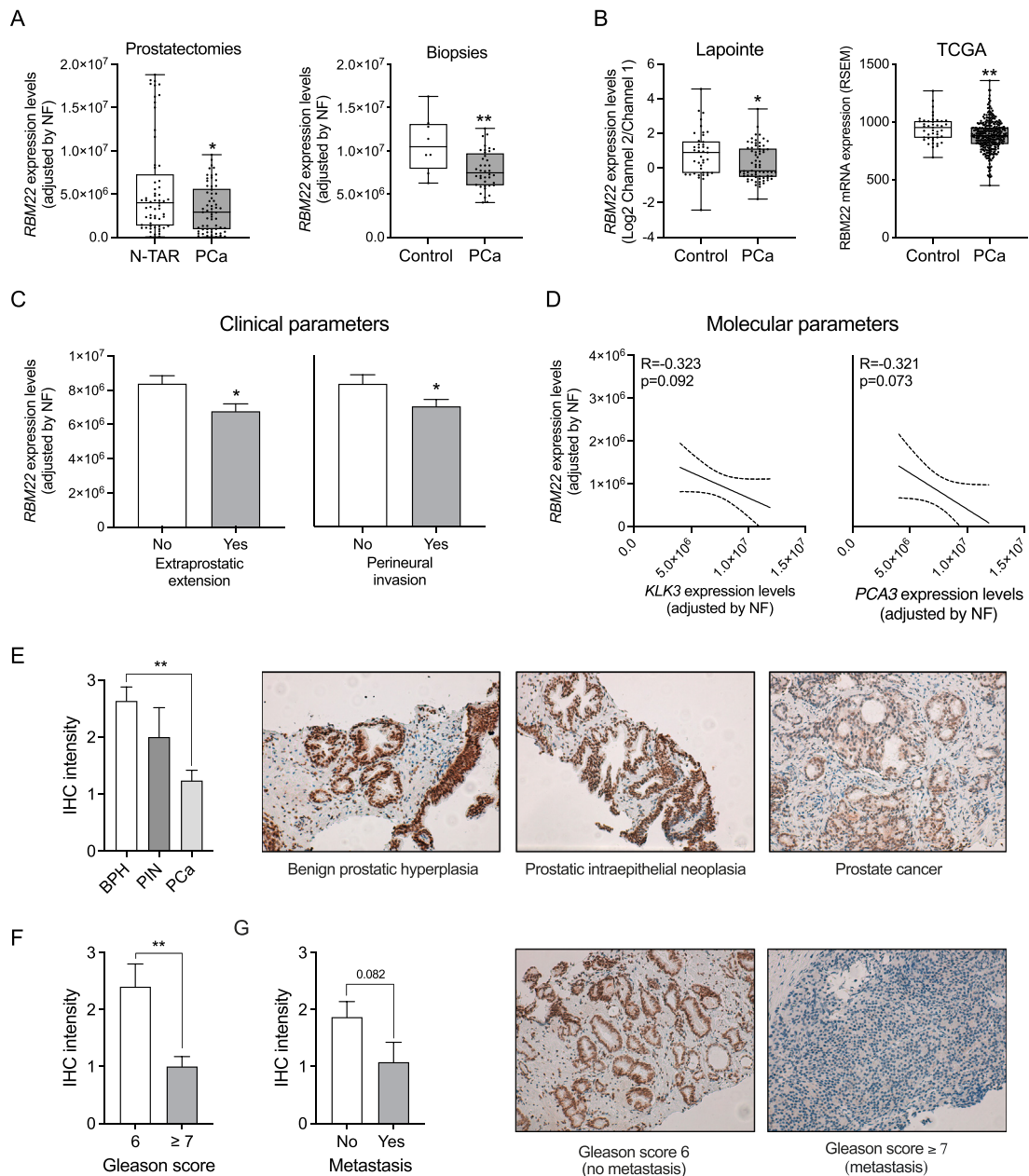


Fig 1. RBM22 levels in human samples. **A**, Comparison of *RBM22* mRNA levels in two cohorts of patients: cohort-1) formalin-fixed paraffin-embedded (FFPE) samples from PCa tissues vs nontumor adjacent regions (N-TAR) (left panel; n = 84); and cohort-2) freshly collected biopsy samples from patients with significant PCa (n = 42) vs nontumor prostate samples (right panel; n = 9). *RBM22* levels were determined by qPCR. Data are represented as mean ± SEM of mRNA levels adjusted by normalization factor (calculated from *ACTB* and *GAPDH* expression levels). **B**, Comparison of *RBM22* mRNA levels from Lapointe (left panel; n = 112) and TCGA (right panel; n = 376) datasets.^{32, 33} Data are represented as mean ± SEM of mRNA levels Log₂ of the ratio of the median of Channel 2 (635 nm) to Channel 1 (532 nm) in Lapointe cohort, and RSEM (Batch normalized from Illumina HiSeq_RNASeqV2) in TCGA cohort. **C**, Association between *RBM22* mRNA levels and clinical parameters (extrastatic extension and perineural invasion) in PCa samples from cohort-2 (n = 42). Data are represented as mean ± SEM of mRNA levels adjusted by normalization factor (calculated from *ACTB* and *GAPDH* expression levels). **D**, Correlation between *RBM22* mRNA levels and expression levels of *KLK3* and *PCA3*. Correlations are represented by mean (connecting line) and error bands (pointed line) of expression levels. **E**, Comparison of *RBM22* protein levels by immunohistochemistry (IHC) between a representative set of benign prostatic hyperplasia (BPH; n = 11), prostatic intraepithelial neoplasia (PIN; n = 6) and prostate cancer (PCa; n = 47) samples (left panel). Representative images (200x magnification) are shown in the right panel. **F**, Association of *RBM22* protein levels with Gleason Score (GS 6 [n = 5] and GS ≥ 7 [n = 42]). **G**, Association of *RBM22* protein levels with presence of metastasis at diagnosis (no metastasis [n = 19] and metastasis [n = 28]). Representative images (200x magnification) are shown in the right panel. Data are represented as mean ± SEM of IHC staining scaled from low¹ to high³ intensity.

and poorly-differentiated prostate cancer (PD-PCA) over time.⁴⁷ Therefore, this model was used to further interrogate *RBM22* levels during PCa progression. We first corroborated that the TRAMP model developed PIN, MD-PCA and PD-PCA at 13, 21 and 30 weeks of age, respectively (Fig 2A). Our results showed that *RBM22* mRNA levels were

significantly lower in MD-PCA and PD-PCA samples compared to PIN samples (Fig 2B). Consistently, a progressive decrease in *RBM22* protein levels was also observed when comparing PIN, MD-PCA, and PD-PCA samples from TRAMP mice (Fig 2C). These findings were also reproduced in the Hi-Myc model (Fig 2,C–E).

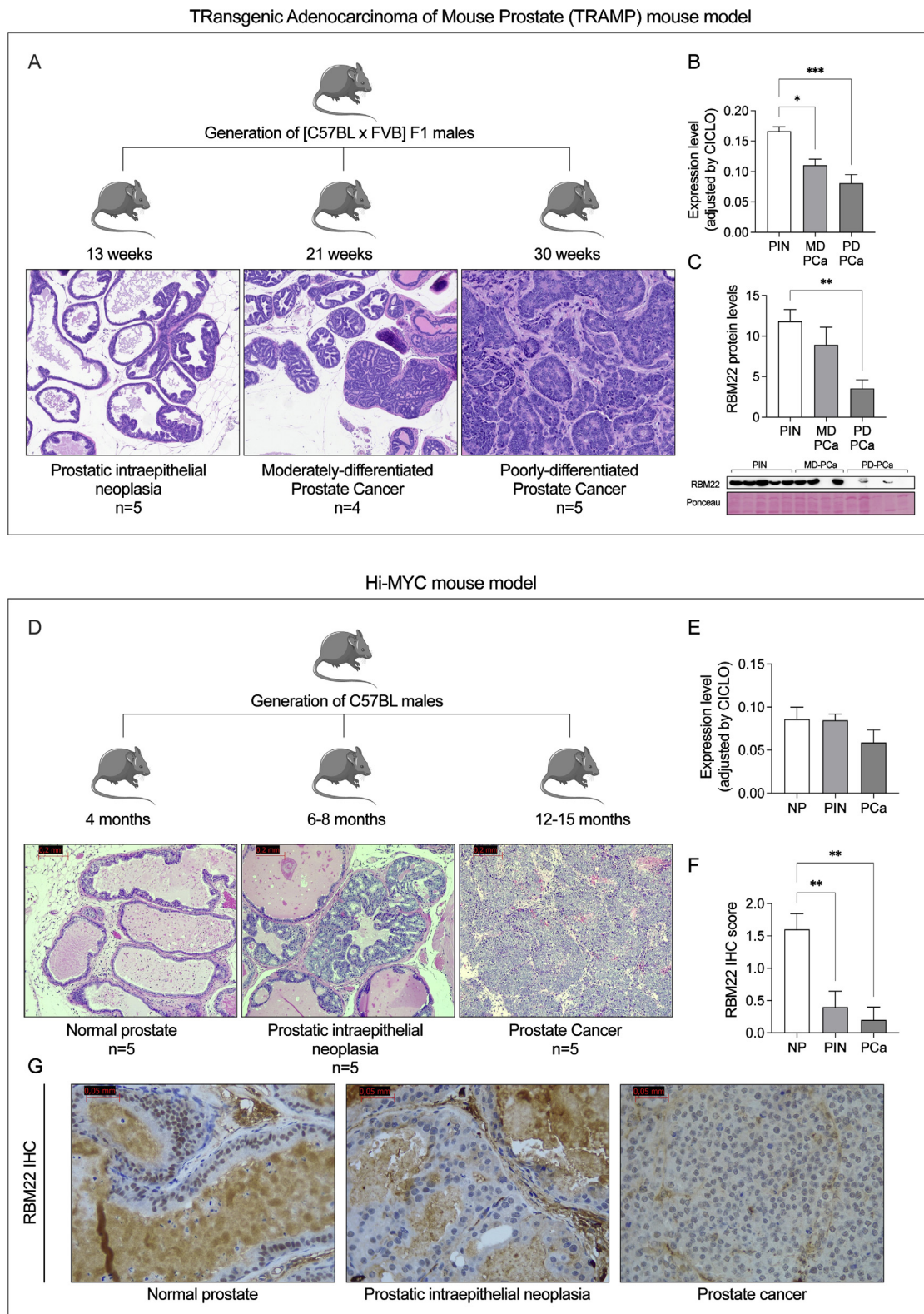


Fig 2. A, Schematic representation of the generation of the preclinical transgenic adenocarcinoma of mouse prostate (TRAMP) model. Representative images of prostatic intraepithelial neoplasia (PIN), moderately-differentiated PCa (MD-PCa) and poorly differentiated PCa (PD-PCa) obtained at 13, 21 and 30 weeks of age from TRAMP mice are shown in the bottom panel, respectively. Images of PIN and MD-PCa are taken with 100x magnification and PD-PCa with 200x magnification. B, Comparison of *RBM22* mRNA levels from PIN (n = 5), MD-PCa (n = 4) and PD-PCa (n = 5) derived from TRAMP mice. Data are represented as mean ± SEM of mRNA levels adjusted by *CICLO* expression levels. Asterisks (* $P < 0.05$; *** $P < 0.001$) indicate statistically significant differences between groups. C, Comparison of *RBM22* protein levels from PIN (n = 5), MD-PCa (n = 4) and PD-PCa (n = 5) derived from TRAMP mice. Protein levels were normalized by total protein loading (Ponceau staining). Asterisks (** $P < 0.01$) indicate statistically significant differences between groups. Western-Blot images of *RBM22* protein levels are included in the right panel.

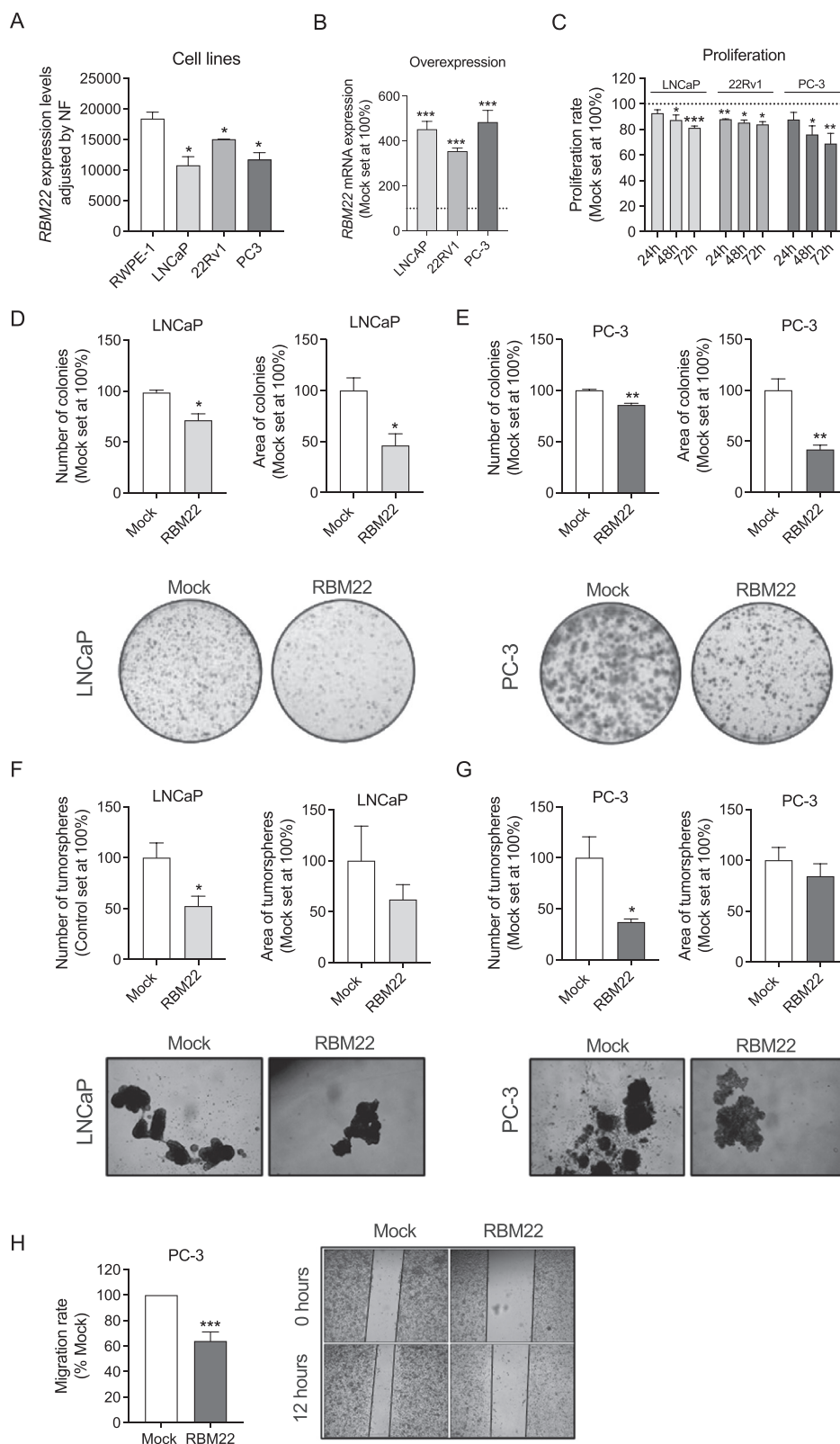


Fig 3. Functional consequences of *RBM22* overexpression in prostate cancer-derived cell lines. **A**, Comparison of *RBM22* mRNA expression levels between non-tumor (RWPE-1) and tumor (22Rv1, LNCaP and PC-3) prostate-derived cell lines. Data are represented as mean \pm SEM of mRNA levels adjusted by normalization factor (calculated from *ACTB* and *GAPDH* expression levels). **B**, Validation of *RBM22* overexpression (by qPCR) in LNCaP, 22Rv1 and PC-3 cell-lines. Data (mean \pm SEM) are represented as percentage of mock-transfected cells (indicated with the dotted line at 100%). *RBM22* expression levels (mRNA) were adjusted by normalization factor (calculated from *ACTB* and *GAPDH* expression levels). **C**, Proliferation rate of LNCaP, 22Rv1 and PC-3 cells in response to *RBM22* overexpression compared to mock-transfected cells (indicated with the dotted line at 100%). Effect of *RBM22* overexpression in LNCaP **D**, and PC-3 **E**, colony number (left panel) and area (right panel) compared to mock-transfected cells. Representative images of LNCaP and PC-3 colonies are depicted on bottom panel. Effect of *RBM22* overexpression in LNCaP **F**,

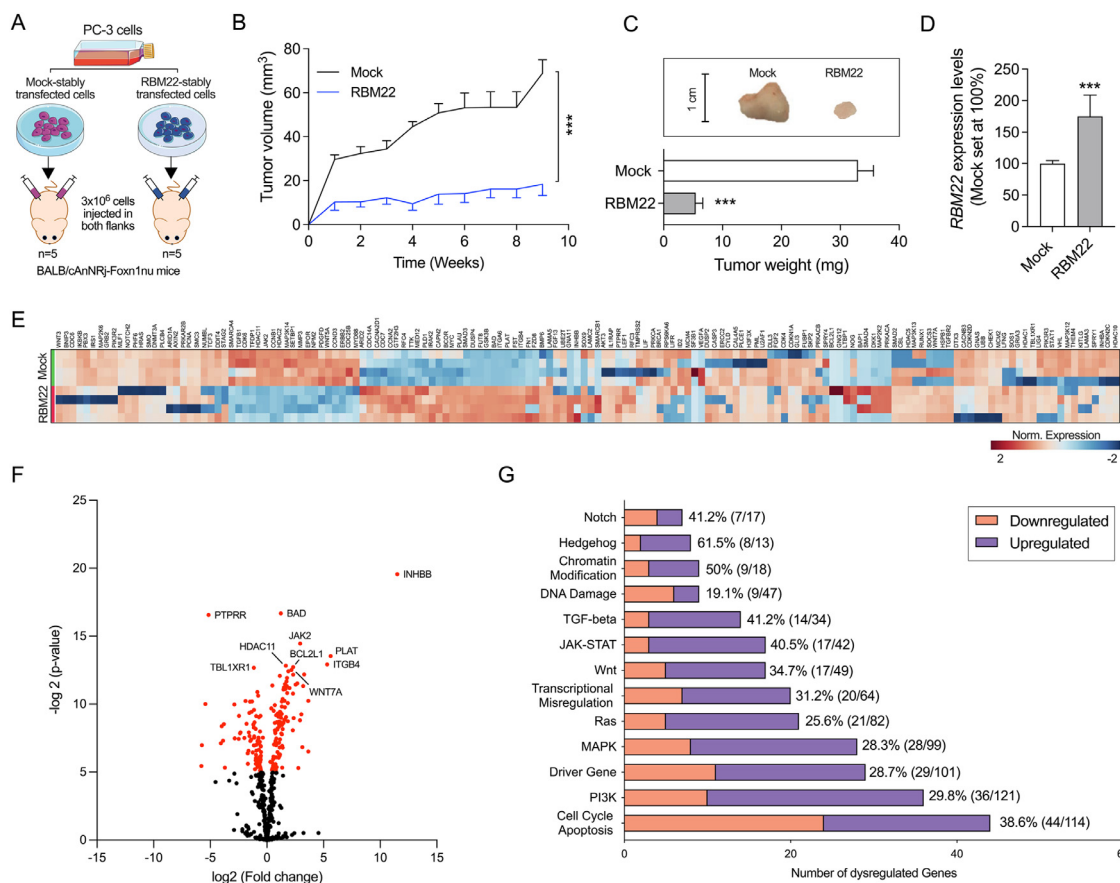


Fig 4. Functional and molecular response to *RBM22* overexpression in a PC-3 xenograft model. **A**, Generation of a preclinical-xenograft PCa-model by subcutaneously inoculating PC-3 cells in one flank cells overexpressing *RBM22* and in the other flank mock-transfected cells (10 tumors/condition). Comparison between the growth over time **B**, and weight at the end of experiment **C**, of xenograft tumors derived from mock-transfected cells and *RBM22*-overexpressing cells. Representative images of tumors are depicted in top panel. **D**, Validation of *RBM22* overexpression by qPCR. mRNA levels were adjusted by normalization factor (calculated from *ACTB* and *GAPDH* expression levels). Data (mean ± SEM) are represented as percentage of mock-transfected xenograft tumors. Asterisks (***) indicate statistically significant differences between groups. **E**, Hierarchical heatmap generated using the expression levels of significantly altered cancer-related genes (154 genes) in *RBM22*-overexpressing (green) vs mock-transfected (red) xenograft tumors. **F**, Volcano plot showing differentially expressed genes (DEGs) in *RBM22*-overexpressing vs mock xenograft tumors. Top 10 significantly altered genes are depicted. Red dots represent statistically significant (P -value < 0.05) and black dots non-significant DEGs. **G**, Cancer-related pathways altered in *RBM22*-overexpressing tumors. Percentage of altered genes, number of dysregulated genes, and total number of genes per pathway are depicted. These expression levels were obtained and analyzed using nCounter PanCancer platform.

Overexpression of RBM22 reduced relevant functional parameters of PCa aggressiveness in vitro

Different human PCa cell-line models (LNCaP, 22Rv1 and PC-3) and a normal-like prostate cell-line (RWPE-1) were used to perform functional experiments. First, *RBM22* expression levels were found to be significantly lower in all the PCa cell lines used herein compared to the normal- prostate cell line RWPE-1 (Fig 3A), indicating that LNCaP, 22Rv1 and PC-3 cell-models were appropriate PCa models to study the functional role of *RBM22*.

Stable overexpression of *RBM22* in LNCaP, 22Rv1 and PC-3 cell lines by transfecting the cells with an *RBM22*-overexpressing plasmid (Fig 3B) resulted in a significant decrease in the proliferation rate at 24-, 48-, and 72-hour in 22Rv1 cells, and at 48-, and 72-hour in LNCaP and PC-3 cells compared with mock-transfected control cells (Fig 3C). Similarly, *RBM22*-overexpressing LNCaP and PC-3 cells generated fewer and smaller colonies than mock-transfected control cells (Fig 3,D and E, respectively). Likewise, the number of tumorspheres was also

significantly decreased in response to *RBM22* overexpression in LNCaP and PC-3 cells, while their size was not affected (Fig 3, F and G, respectively). Finally, given its high invasiveness nature, the role of *RBM22* on migration capacity was explored in PC-3 cells.³⁹ Our results showed that *RBM22* overexpression markedly decreased the migration rate of PC-3 cells after 12 hours (Fig 3H). All these results revealed that *RBM22* overexpression affected different critical functional endpoints associated with the development, progression, and aggressiveness of PCa cells.

Overexpression of RBM22 impairs PCa progression in vivo by the modulation of critical signaling pathways in PCa

To validate the *RBM22* antitumor actions *in vivo*, we generated another preclinical model to monitor the growth of xenograft PC-3 tumors overexpressing *RBM22* compared to mock-transfected PC-3 cells (Fig 4A). Specifically, analysis of tumor growth showed that PCa progression *in vivo* was completely blunted in *RBM22*-overexpressing tumors vs control (mock-transfected) tumors (Fig 4B). Consistently,

and PC-3 G, tumorsphere number (left panel) and area (right panel) compared to mock-transfected cells. Representative images of LNCaP and PC-3 tumorspheres are depicted on bottom panel. **H**, Migration rate of PC-3 cells in response to *RBM22* overexpression compared to mock-transfected cells. Representative images are depicted on right panel. Asterisks (* P < 0.05; ** P < 0.01; *** P < 0.001) indicate statistically significant differences between groups.

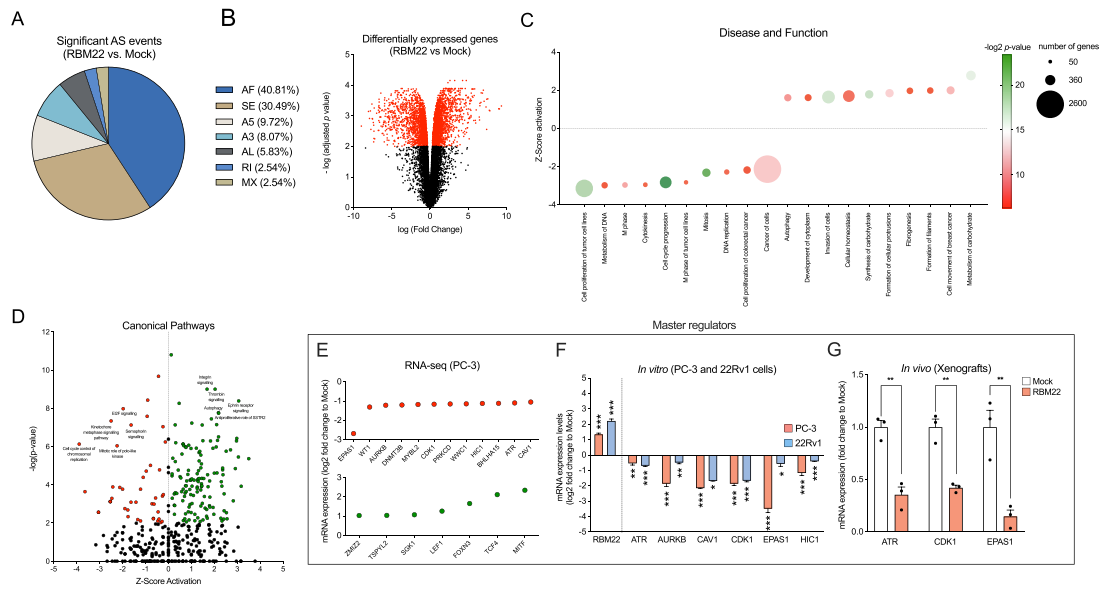


Fig 5. Molecular and signaling landscape in response to *RBM22* overexpression in PCa cells. **A**, Distribution of splicing events significantly altered in *RBM22*-overexpressing vs mock PC-3 cells (AF: Alternative First Exon; SE: Exon skipping; A5: Alternative 5' Splice Site; A3: Alternative 3' Splice Site; AL: Alternative Last Exon; RI: Intron retention; MX: Mutually Exclusive Exon). **B**, Volcano plot showing differentially expressed genes in *RBM22*-overexpressing vs mock-overexpressing PC-3 cells. Red dots represent statistically significant and black dots non-significant differentially expressed genes (DEGs), respectively. **C**, Activation status of disease and function pathways enriched in *RBM22*-overexpressing PC-3 cells. Top 10 most-activated and top 10 least-activated pathways are depicted. **D**, Activation status of canonical pathways enriched in *RBM22*-overexpressing PC-3 cells. Red blots represent canonical pathways significantly inhibited and green blots represent canonical pathways significantly activated in *RBM22*-overexpressing PC-3 cells. Black dots represent non-significantly enriched pathways. **(E-G)**, Analysis of the expression levels of master regulators in response to *RBM22* overexpression. **E**, Differentially expressed master regulators in *RBM22*-overexpressing PC-3 cells (data from RNAseq). Red blots represent downregulated and green dots upregulate genes in *RBM22*-overexpressing PC-3 cells. **F**, Master regulators differentially expressed in response to *RBM22* overexpression in 3 independent biological replicates from PC-3 and 22Rv1 cells. **G**, Expression levels of differentially expressed master regulators in PC-3 xenografts overexpressing *RBM22*. Data (mean ± SEM) are represented as fold change of mock-transfected xenograft tumors. Asterisks (* $P < 0.05$; ** $P < 0.01$; *** $P < 0.001$) indicate statistically significant differences between groups. “(For interpretation of the references to color in this figure legend, the reader is referred to the Web version of this article.)”

overexpression of *RBM22* *in vivo* resulted in smaller tumors as compared to mock-cells induced tumors (Fig. 4C). It should be mentioned that *RBM22* overexpression was validated at the end of the experiment in the harvested tumors (Fig. 4D).

Overexpression of *RBM22* *in vivo* altered the expression of 154 out of 770 genes analyzed using the nCounter PanCancer Pathways Panel kit (Fig 4, E and F). Specifically, cell cycle-apoptosis pathway was the most altered signaling pathway, followed by PI3K pathway and driver gene pathway (Fig 4G). Additionally, other critical signaling pathways were also altered, including MAPK, Ras, transcription misregulation, Wnt and JAK-STAT pathways, among others (Fig 4G).

Molecular landscape in response to RBM22 overexpression revealed that RBM22 regulates the splicing pattern of critical genes and the activity of oncogenic signaling pathways in PCa cells

Given the pivotal role of AR in PCa progression⁵ together with previous studies reporting a causal link between SFs and AR pathway,^{19,49,50} the potential relationship between *RBM22* and AR was investigated herein in LNCaP (hypersensitive to AR stimulation, AR⁺/AR-V7⁻) and 22Rv1 (AR⁺/AR-V7⁺) cells.⁵¹⁻⁵³ Specifically, DHT treatment did not dysregulate *RBM22* levels in LNCaP cells (Supplemental Figure 4A). In addition, *RBM22* overexpression did not alter *AR* nor *AR-V7* levels in LNCaP and 22Rv1 cells (Supplemental Figure 4B-D). Then, an unbiased approach was followed, a RNAseq analysis in *RBM22*-overexpressing PC-3 cells. This transcriptome analysis revealed that *RBM22* overexpression dysregulated the splicing pattern of 397 genes by altering 669 alternative splicing events, being alternative first exon and exon skipping the most common events (41% and 30%, respectively; Fig 5A and Supplemental Figure 5). Moreover, according to its role as a potential transcription factor, the overexpression of *RBM22* altered the expression levels of

4245 genes with an adjusted *P*-value < 0.01 (Fig 5B; Supplemental Table 2). Specifically, disease and function pathways analyses showed that cell cycle progression was the most significantly inactivated pathway in response to *RBM22* overexpression (Fig 5C). In addition, *RBM22* overexpression decreased the activity of other key pathways tightly related to cell cycle, including cell proliferation of tumor cell lines, metabolism of DNA, M phase, Cytokinesis, M phase of tumor cell lines, Mitosis, DNA replication and cancer cells, among others (Fig 5C, Supplemental Table 3). On the other hand, overexpression of *RBM22* was associated to high activity of autophagy, development of cytoplasm, invasion of cells and cellular homeostasis among others (Fig 5C, Supplemental Table 3).

Consistently, the transcriptional landscape predicted 216 canonical pathways that were altered in *RBM22*-overexpressing PC-3 cells. Specifically, *RBM22* overexpression decreased the activation of key oncogenic pathways involved in cell cycle regulation including cell cycle control of chromosomal replication, kinetochore metaphase signaling pathway, mitotic role of polo-like kinase, and semaphorin pathway, among others (Fig 5D; Supplemental Table 4). Similarly, *RBM22* overexpression also decreased the activation of antioncogenic pathways, including ephrin receptor, antiproliferative role of SSTR2, integrin signaling, thrombin signaling, and autophagy pathway, among others (Fig 5D; Supplemental Table 4).

Transcriptional changes in *RBM22*-overexpressing cells were further analysed to interrogate the expression levels of master regulators and therefore identify the main molecular drivers underlying the antitumor role of *RBM22* in PCa cells. Specifically, RNAseq data showed that *EPAS1*, *WT1*, *AURKB*, *DNMT3B*, *MYBL2*, *CDK1*, *PRKCD*, *WWC1*, *HIC1*, *BHLHA15*, *ATR* and *CAV1* were downregulated, while *ZMIZ2*, *TSPYL2*, *SGK1*, *LEF1*, *FOXN2*, *TCF4*, and *MITF* were upregulated in response to *RBM22* overexpression in PC-3 cells (Fig 5E). Changes in the expression levels of *ATR*, *AURKB*, *CAV1*, *CDK1*, *EPAS1* and *HIC1* were further validated by RT-

qPCR in PC-3 and 22Rv1 using 3 independent biological replicates (Fig 5F; Supplemental Figure 6A-6C). Finally, the decrease in the expression levels of *ATR*, *CDK1* and *EPAS1* in response to *RBM22* expression was also validated in the preclinical xenograft *in vivo* mouse-model (Fig 5G).

Discussion

RNA binding motif (RBM) proteins represent a complex family comprised by proteins that can either fuel cancer progression or suppress tumor development and/or progression.^{54,55} Molecularly, although the main function of RBM proteins is the regulation of splicing process,⁵⁴ some of them can also regulate transcription, therefore controlling a plethora of signaling pathways.^{28,56} This is the case of *RBM22*, which has an RNA Recognition Motif (RRM) but also a Zinc-Finger like domain.²⁸ As other members of the RBM family, the role of *RBM22* in cancer seems to be context-dependent, inasmuch as *RBM22* has been found to be overexpressed in glioblastoma multiforme,¹⁷ but lost in myelodysplastic syndrome (ie precursor of acute myeloid leukemia).⁵⁷

Surprisingly, although many splicing factors have been found to be dysregulated and play a key role in the development, progression and treatment resistance of PCa,^{19,20,58} the levels and potential pathophysiological actions that *RBM22* might play in this tumor type remain completely unknown. Therefore, we herein evaluated the levels of *RBM22* and interrogated its potential functional role in PCa, one of the top leading causes of cancer-related deaths among male population in developed countries,¹ which is still lacking global therapeutic targets that could lead to more effective therapeutic approaches. In this sense, our results showed that the expression of *RBM22* was downregulated in PCa samples from 3 cohorts of samples available at our laboratory and 2 publicly available datasets. Interestingly, *RBM22* protein levels were especially low in highly aggressive PCa samples (ie Gleason score ≥ 7 , extra prostatic extension and perineural invasion), suggesting a potential tumor suppressor role for this protein in PCa. Consistently, *RBM22* decreased (at mRNA and protein level) gradually from PIN to poorly differentiated PCa in samples from TRAMP mice (a transgenic model that closely mimics human PCa progression)⁴⁷, thus reinforcing the link between low *RBM22* levels and PCa progression and aggressiveness.

Given that *RBM22* was significantly downregulated in all the PCa models tested herein (ie cell lines as well as tumors from the TRAMP and Hi-MYC mice), our approach to study the potential pathophysiological role of *RBM22* in PCa consisted in overexpressing *RBM22* in LNCaP and 22Rv1 (AR driven cells) as well as in PC-3 (AR-independent cells). Specifically, *RBM22* overexpression decreased aggressiveness features of these PCa cell-lines, including cell proliferation and migration. In addition, *RBM22* overexpression also strikingly decreased PCa-stem/progenitor cells in terms of tumorspheres and colonies number and/or area, both relevant functional results that may help to explore the PCa-onset and how to overcome the well-known PCa-resistance to different/current drugs.^{59,60} Consistently, we also demonstrated the antitumor actions of *RBM22 in vivo* by generating a preclinical model, since tumor progression was completely blocked in xenografted *RBM22*-overexpressing tumors (ie tumor grew dramatically slower and tumor weight was significantly lower than mock-transfected control tumors). Thus, all these robust *in vitro/in vivo* results, together with the observations using 5 different human cohorts, unveiled an important pathophysiological role of *RBM22* in PCa. Specifically, these results indicate that *RBM22* plays an antitumor role in PCa cells, which is consistent with previous studies showing that *RBM3*, *RBM5* and *RBM25* act as tumor suppressors in PCa and are inversely related to PCa aggressiveness.^{21,22,61} In this sense, it has been reported that 5q33.1, the chromosome region harboring *RBM22* gene, is commonly lost in Afro-American patients as compared to Caucasian patients.⁶² In this context, it is widely known that prostate tumors derived from Afro-American patients are usually more aggressive than those derived from Caucasian patients,^{63,64} whether *RBM22* loss is a player involved in Afro-American PCa oncogenesis and aggressiveness remains unknown, but our data open a new research

avenue on that direction and suggest that *RBM22*-overexpression could be a novel therapeutic avenue with relevant pathophysiological/clinical-potential, to combat this devastating disease.

Therefore, our data lay the foundations to further study *RBM22* biology in order to unveil the molecular and signaling mechanisms underlying the decrease in its expression levels in advanced PCa, and therefore identify novel therapeutic targets to tackle this lethal disease. In this regard, although *RBM22* copy number alterations associated with *RBM22* mRNA levels in the cohorts analyzed herein, many diploid samples exhibited low mRNA levels of *RBM22*, similar to those observed in samples harboring *RBM22* shallow or deep deletions. Moreover, differences in *RBM22* levels between PCa and non-tumor tissues were more pronounced at protein levels compared to mRNA levels. These data might suggest that the downregulation of *RBM22* observed in PCa could be due in part to *RBM22* shallow deletions, but in a more extent to an alteration in the transcriptomic rate/efficiency of *RBM22* gene (eg, epigenetic changes) and/or to the dysregulation of *RBM22* translation efficiency or protein stability. In this sense, many studies have reported a potential key role that proteins involved in ubiquitination and deubiquitination of SFs (E3-ligases and deubiquitinating enzymes) play to regulate splicing process.⁶⁵⁻⁶⁷ However, further studies are needed to fully address the molecular mechanisms driving *RBM22* downregulation in PCa.

Mechanistically, *RBM22* has been found to shuttle between the nucleus and the cytoplasm in response to cellular stress conditions in other cell-types (regulating Calcium signaling through the interaction with ALG-2 and SLU7).^{68,69} Nevertheless, our data showed that *RBM22* protein staining was restricted to the nuclei of the tumor cells, which suggest that the main processes regulated by *RBM22* in PCa cells might be alternative splicing and gene transcription. According to this observation we aimed to identify the splicing events differentially processed and the genes differentially expressed in response to *RBM22* overexpression. To that aim, RNA from *RBM22*-overexpressing and mock-transfected PC-3 cells were used. Our data demonstrated that *RBM22* overexpression triggers a profound alteration in the splicing pattern of 856 genes, which is plausible considering the pivotal role that *RBM22* plays in the activation of the spliceosome.²⁵ Interestingly, among all the types of splicing events, exon skipping, and alternative last exon were the most commonly altered ones in response to *RBM22* overexpression. On the other hand, Van Nostrand et al. showed that intron retention and exon skipping were the top-altered alternative splicing events in response to *RBM22* knockdown in K-562 and HepG2 cells,²⁷ which might suggest that *RBM22* modulation in terms of splicing landscape could be cell-type dependent, and might be one of the reasons underlying the distinct role of *RBM22* in different cancer-types.

Apart from its role as a regulator of the splicing process, it has been reported that *RBM22* can also regulate gene transcription, presumably acting as a transcription factor through its Zinc-Finger like domain.²⁸ In line with this, we found 4245 genes differentially expressed in response to *RBM22* overexpression in PCa cells, pointing out its role as transcription regulator. Then, to unveil the molecular mechanisms underlying the antitumor role of *RBM22* in PCa cells, pathways enrichment analysis was done with the transcriptional landscape of *RBM22*-overexpressing PC-3 cells, using IPA software. Specifically, *RBM22* overexpression was associated with the dysregulation of various critical pathways, including the inhibition of cell cycle progression. In fact, results from nCounter Pan-Cancer Pathways Panel array performed in *RBM22*-overexpressing and mock-transfected xenograft tumors corroborated the relation of *RBM22* with cell cycle progression. Therefore, our data suggest that high *RBM22* levels lead to cell cycle arrest in PCa cells. Indeed, bioinformatics analyses using IPA software identified *CDK1* as one of the master regulators driving the effects of *RBM22* in PCa, which is widely known to be an essential player driving cell cycle.⁷⁰ Specifically, *CDK1* interacts with *CCNB1*, which we also found to be downregulated in response to *RBM22 in vitro* and *in vivo*, to form the maturation-promoting factor, a complex that is necessary for the proper control of the G2/M transition phase of the cell cycle.⁷¹ In addition, *EPAS1* (also known as *HIF2a*) was also found herein

to be another master regulator of RBM22 effects in PCa. Remarkably, EPAS1 has been reported to be upregulated in PCa and positively correlated with androgen receptor expression.⁷² Importantly, EPAS1 transcriptionally upregulates tumorigenic hypoxia-responsive genes (ie VEGF), representing a key factor driving angiogenesis, but being also involved in cell proliferation.⁷³ Finally, our data demonstrated that downregulation of *ATR*, an essential regulator of genome integrity,⁷⁴ is another key molecular event in response to *RBM22* overexpression (see graphical abstract).

Remarkably, these molecular changes driven by *RBM22* dysregulation might be clinically exploitable. Specifically, it is widely known that *CDK1* induces DNA homologous recombination repair (HR) by recruiting Rad51 to DNA damage sites.⁷⁵ Consistently, it has been reported that *CDK1* inhibition reduces HR activity and causes synthetic lethal damage in *BRCA* proficient cells combined with *PARP* inhibitors.⁷⁶ In addition, *PARP* and *ATR* dual inhibition has been shown to synergistically reduce tumor aggressiveness, and even to overcome *PARP* inhibition resistance, *in vitro* and *in vivo* in different tumor-types, including PCa.^{77–79} Therefore, given that we demonstrated herein that stably overexpression of *RBM22* led to a dramatic decrease in *CDK1* and *ATR* expression levels in PCa cells, it is tempting to suggest that *RBM22*-overexpressing tumors might benefit from the therapeutic intervention with *PARP* inhibitors (eg, Olaparib, rucaparib). However, this hypothesis should be taken with caution since to date only HR gene mutations (especially in *BRCA1/2*) has been associated with response to *PARP* inhibitors (especially in *mCRPC*).^{80,81} Therefore, despite the promising preclinical data,^{76–79} no clinical studies have proven the predictive value of any transcriptional HRR signature yet.

Taken together, our data unveiled new conceptual and functional avenues in PCa, with potential clinical implications, by demonstrating that *RBM22* has a critical functional role in the pathophysiology of PCa since its overexpression impaired key pathophysiological processes in PCa-biology (ie proliferation, migration, tumorspheres and colonies formation) likely by modulating critical oncogenic signaling pathways associated with PCa initiation/progression/aggressiveness. Moreover, our results pave the way to study negative regulators of *RBM22* that could become potential therapeutic targets, as well as invites to suggest that *RBM22* levels might represent a biomarker of response to *PARP* inhibitors, offering a clinically relevant therapeutic opportunity that should be further explored and ultimately tested in humans.

Acknowledgments

Conflicts of Interest: All authors have read the journal's policy on disclosure of potential conflicts of interest and have none to declare.

This research was funded by the Spanish Ministry of Science, Innovation, and Universities (Research–Grant: [PID2019–105564RB–I00](#); Pre-doctoral contracts: [FPU16/05059](#), [FPU17/00263](#), [FPU18/02485](#)), Health Institute Carlos III ([DTS20-00050](#)), Junta de Andalucía [[BIO-0139](#)]; Consejería de Transformación Económica, Industria, Conocimiento y Universidades ([P20_00442](#)); Consejería de Salud y Familias, co-funded by European Union (Programa Operativo FEDER de Andalucía 2014-2020, “Andalucía se mueve con Europa”: [PEER-0048-2020](#)), and CIBERobn (CIBER is an initiative of Instituto de Salud Carlos III, Ministerio de Sanidad, Servicios Sociales e Igualdad, Spain). Funding for open access charge: University of Córdoba/CBUA. Some images were taken from Servier Medical Art (smart.servier.com) under the Creative Commons Attribution 3.0 Unported License. Special thanks to the staff of Biobank of the IMIBIC and of the experimental animal service (SAE) of the UCO/IMIBIC. We are gratefully indebted to all the patients and their families for generously donating the samples and clinical data for research purposes. All authors have read the journal's authorship agreement.

Author contributions are as follow: JMJV contributed to the conception of the work, design of the work, acquisition, analysis and interpretation of the data and drafted the work; AJMH contributed to the conception of the work, design of the work, acquisition, analysis and interpretation of the data and drafted the work; EGG contributed to the

acquisition, analysis and interpretation of the data; PSM contributed to the acquisition and analysis of the data; ACFF contributed to the acquisition and analysis of the data; AC contributed to the analysis of the data; TGS contributed to the acquisition and analysis of the data; AML contributed to the acquisition and analysis of the data; RSS- contributed to the acquisition and analysis of the data; PPLC contributed to the acquisition of the data; ASC contributed to the acquisition of the data; DO contributed to the acquisition and interpretation of the data and substantively revised the work; EE contributed to the acquisition and interpretation of the data and substantively revised the work; JPC contributed to the acquisition and interpretation of the data and substantively revised the work; MDG contributed to the design of the work, acquisition and interpretation of the data and substantively revised the work; RMLH contributed to the conception of the work, design of the work, acquisition, analysis and interpretation of the data, drafted and substantively revised the work.

Data statement: The datasets used and/or analyzed during the current study are available in this article and/or available from the corresponding author on reasonable request.

Supplementary materials

Supplementary material associated with this article can be found in the online version at [doi:10.1016/j.trsl.2022.08.016](https://doi.org/10.1016/j.trsl.2022.08.016).

References

- Bray F, Ferlay J, Soerjomataram I, Siegel RL, Torre LA, Jemal A. Global cancer statistics 2018: GLOBOCAN estimates of incidence and mortality worldwide for 36 cancers in 185 countries. *CA Cancer J Clin* 2018;68(6):394–424.
- Tolkach Y, Kristiansen G. The heterogeneity of prostate cancer: a practical approach. *Pathobiology* 2018;85(1–2):108–16.
- Sandhu S, Moore CM, Chiong E, Beltran H, Bristow RG, Williams SG. Prostate cancer. *Lancet* 2021;398(10305):1075–90.
- Sartor O, de Bono JS. Metastatic prostate cancer. *N Engl J Med* 2018;378(7):645–57.
- Westaby D, Fenor de La Maza MLD, Paschalis A, et al. A new old target: androgen receptor signaling and advanced prostate cancer. *Annu Rev Pharmacol Toxicol* 2022;62:131–53.
- Mateo J, Seed G, Bertan C, et al. Genomics of lethal prostate cancer at diagnosis and castration resistance. *J Clin Invest* 2020;130(4):1743–51.
- Fraser M, Sabelnykova VY, Yamaguchi TN, et al. Genomic hallmarks of localized, non-indolent prostate cancer. *Nature* 2017;541(7637):359–64.
- Cooper CS, Eeles R, Wedge DC, et al. Analysis of the genetic phylogeny of multifocal prostate cancer identifies multiple independent clonal expansions in neoplastic and morphologically normal prostate tissue. *Nat Genet* 2015;47(4):367–72.
- Boutros PC, Fraser M, Harding NJ, et al. Spatial genomic heterogeneity within localized, multifocal prostate cancer. *Nat Genet* 2015;47(7):736–45.
- Ladomery M. Aberrant alternative splicing is another hallmark of cancer. *Int J Cell Biol* 2013;2013:463786.
- Oltean S, Bates DO. Hallmarks of alternative splicing in cancer. *Oncogene* 2014;33(46):5311–8.
- Rahman MA, Krainer AR, Abdel-Wahab O. SnapShot: splicing alterations in cancer. *Cell* 2020;180(1):208–e1.
- Jimenez-Vacas JM, Herrero-Aguayo V, Montero-Hidalgo AJ, et al. Dysregulation of the splicing machinery is directly associated to aggressiveness of prostate cancer. *EBioMedicine* 2020:102547.
- Jimenez-Vacas JM, Herrero-Aguayo V, Gomez-Gomez E, et al. Spliceosome component SF3B1 as novel prognostic biomarker and therapeutic target for prostate cancer. *Transl Res* 2019;212:89–103.
- Hormaechea-Agulla D, Jimenez-Vacas JM, Gomez-Gomez E, et al. The oncogenic role of the spliced somatostatin receptor sst5TMD4 variant in prostate cancer. *Faseb J* 2017;31(11):4682–96.
- Hormaechea-Agulla D, Gahete MD, Jimenez-Vacas JM, et al. The oncogenic role of the In1-ghrelin splicing variant in prostate cancer aggressiveness. *Mol Cancer* 2017;16(1):146.
- Fuentes-Fayos AC, Vazquez-Borrego MC, Jimenez-Vacas JM, et al. Splicing machinery dysregulation drives glioblastoma development/aggressiveness: oncogenic role of SRSF3. *Brain* 2020;143(11):3273–93.
- Fuentes-Fayos AC, Perez-Gomez JM, GG ME, et al. SF3B1 inhibition disrupts malignancy and prolongs survival in glioblastoma patients through BCL2L1 splicing and mTOR/ss-catenin pathways imbalances. *J Exp Clin Cancer Res* 2022;41(1):39.
- Paschalis A, Sharp A, Welti JC, et al. Alternative splicing in prostate cancer. *Nat Rev Clin Oncol* 2018;15(11):663–75.
- Takayama KI. Splicing factors have an essential role in prostate cancer progression and androgen receptor signaling. *Biomolecules* 2019;9(4):131.
- Zeng Y, Wodzinski D, Gao D, et al. Stress-response protein RBM3 attenuates the stem-like properties of prostate cancer cells by interfering with CD44 variant splicing. *Cancer Res* 2013;73(13):4123–33.

22. Zhao L, Li R, Shao C, Li P, Liu J, Wang K. 3p21.3 tumor suppressor gene RBM5 inhibits growth of human prostate cancer PC-3 cells through apoptosis. *World J Surg Oncol* 2012;10:247.
23. Yamamoto R, Osawa T, Sasaki Y, et al. Overexpression of p54(nrb)/NONO induces differential EPHA6 splicing and contributes to castration-resistant prostate cancer growth. *Oncotarget* 2018;9(12):10510–24.
24. Takayama KI, Suzuki T, Fujimura T, et al. Dysregulation of spliceosome gene expression in advanced prostate cancer by RNA-binding protein PSF. *Proc Natl Acad Sci U S A* 2017;114(39):10461–6.
25. Rasche N, Dybkov O, Schmitzova J, Akyildiz B, Fabrizio P, Luhrmann R. Cwc2 and its human homologue RBM22 promote an active conformation of the spliceosome catalytic centre. *EMBO J* 2012;31(6):1591–604.
26. Rasche N, Dybkov O, Schmitzová J, Akyildiz B, Fabrizio P, Luhrmann R. Cwc2 and its human homologue RBM22 promote an active conformation of the spliceosome catalytic centre. *EMBO J* 2012;31(6):1591–604.
27. Van Nostrand EL, Freese P, Pratt GA, et al. A large-scale binding and functional map of human RNA-binding proteins. *Nature* 2020;583(7818):711–9.
28. Xiao R, Chen JY, Liang Z, et al. Pervasive chromatin-RNA binding protein interactions enable RNA-based regulation of transcription. *Cell* 2019;178(1): 107–21.e18.
29. Soubise B, Jiang Y, Douet-Guilbert N, Troadec MB. RBM22, a key player of Pre-mRNA splicing and gene expression regulation, is altered in Cancer. *Cancers (Basel)* 2022;14(3):643.
30. Gao J, Aksoy BA, Dogrusoz U, et al. Integrative analysis of complex cancer genomics and clinical profiles using the cBioPortal. *Sci Signal* 2013;6(269):11.
31. Cerami E, Gao J, Dogrusoz U, et al. The cBio cancer genomics portal: an open platform for exploring multidimensional cancer genomics data. *Cancer Discov* 2012;2(5):401–4.
32. Lapointe J, Li C, Higgins JP, et al. Gene expression profiling identifies clinically relevant subtypes of prostate cancer. *Proc Natl Acad Sci U S A* 2004;101(3):811–6.
33. Cancer Genome Atlas Research Network. The molecular taxonomy of primary prostate Cancer. *Cell* 2015;163(4):1011–25.
34. Abida W, Cyrta J, Heller G, Prandi D, Armenia J, Coleman I, et al. Genomic correlates of clinical outcome in advanced prostate cancer. *Proc Natl Acad Sci U S A* 2019;116(23):11428–36.
35. Sáez-Martínez P, Jiménez-Vacas JM, León-González AJ, Herrero-Aguayo V, Montero Hidalgo AJ, Gómez-Gómez E, et al. Unleashing the diagnostic, prognostic and therapeutic potential of the neuronostatin/GPR107 system in prostate cancer. *J Clin Med* 2020;9(6):1703.
36. Jimenez-Vacas JM, Gomez-Gomez E, Montero-Hidalgo AJ, et al. Clinical utility of ghrelin-O-Acyltransferase (GOAT) enzyme as a diagnostic tool and potential therapeutic target in prostate cancer. *J Clin Med* 2019;8(12):2056.
37. Gómez-Gómez E, Jiménez-Vacas JM, Pedraza-Arévalo S, et al. Oncogenic role of secreted engrailed homeobox 2 (EN2) in prostate Cancer. *J Clin Med* 2019;8(9):1400.
38. Vandesompele J, De Preter K, Pattyn F, et al. Accurate normalization of real-time quantitative RT-PCR data by geometric averaging of multiple internal control genes. *Genome Biol* 2002;3(7). RESEARCH0034.
39. Su ZZ, Lin J, Shen R, Fisher PE, Goldstein NI, Fisher PB. Surface-epitope masking and expression cloning identifies the human prostate carcinoma tumor antigen gene PCTA-1 a member of the galectin gene family. *Proc Nat Acad Sci of the U S A* 1996;93(14):7252–7.
40. Del Rio-Moreno M, Alors-Perez E, Borges de Souza P, et al. Peptides derived from the extracellular domain of the somatostatin receptor splicing variant SST5TMD4 increase malignancy in multiple cancer cell types. *Transl Res* 2019;211:147–60.
41. Frankish A, Diekhans M, Ferreira AM, et al. GENCODE reference annotation for the human and mouse genomes. *Nucleic Acids Res* 2019;47(D1):D766–D73.
42. Patro R, Duggal G, Love MI, Irizarry RA, Kingsford C. Salmon provides fast and bias-aware quantification of transcript expression. *Nature methods* 2017;14(4):417–9.
43. Sonesson C, Love MI, Robinson MD. Differential analyses for RNA-seq: transcript-level estimates improve gene-level inferences. *F1000Res* 2015;4:1521.
44. Ritchie ME, Phipson B, Wu D, et al. limma powers differential expression analyses for RNA-sequencing and microarray studies. *Nucleic Acids Res* 2015;43(7):e47.
45. Trincado JL, Entizne JC, Hysenaj G, et al. SUPPA2: fast, accurate, and uncertainty-aware differential splicing analysis across multiple conditions. *Genome Biol* 2018;19(1):40.
46. Alamancos GP, Pages A, Trincado JL, Bellora N, Eyras E. Leveraging transcript quantification for fast computation of alternative splicing profiles. *RNA* 2015;21(9):1521–31.
47. Gelman IH. How the TRAMP model revolutionized the study of prostate Cancer progression. *Cancer Res* 2016;76(21):6137–9.
48. Sarmento-Cabral A, F LL, Gahete MD, Castano JP, Luque RM. Metformin reduces prostate Tumor growth, in a diet-dependent manner, by modulating multiple signaling pathways. *Molecular cancer research: MCR* 2017;15(7):862–74.
49. Munkley J, Li L, Krishnan SRG, et al. Androgen-regulated transcription of ESRP2 drives alternative splicing patterns in prostate cancer. *Elife* 2019;8: e47678.
50. Paschalis A, Welti J, Neeb AJ, et al. JMJD6 Is a Druggable oxygenase that regulates AR-V7 expression in prostate Cancer. *Cancer Res* 2021;81(4):1087–100.
51. Horoszewicz JS, Leong SS, Kawinski E, et al. LNCaP model of human prostatic carcinoma. *Cancer Res* 1983;43(4):1809–18.
52. Sramkoski RM, Pretlow 2nd TG, Giaconia JM, et al. A new human prostate carcinoma cell line, 22Rv1. *In Vitro Cell Dev Biol Anim* 1999;35(7):403–9.
53. Sowalsky AG, Figueiredo I, Lis RT, et al. Assessment of Androgen receptor splice variant-7 as a biomarker of clinical response in castration-sensitive prostate cancer. *Clin Cancer Res* 2022;28:3509–25.
54. Li Z, Guo Q, Zhang J, et al. The RNA-binding motif protein family in cancer: friend or foe? *Front Oncol* 2021;11:757135.
55. Dvinge H, Kim E, Abdel-Wahab O, Bradley RK. RNA splicing factors as oncoproteins and tumour suppressors. *Nat Rev Cancer* 2016;16(7):413–30.
56. De Maio A, Yalamanchili HK, Adamski CJ, et al. RBM17 interacts with U2SURP and CHERP to regulate expression and splicing of RNA-processing proteins. *Cell Rep* 2018;25(3): 726–36.e7.
57. Boulwood J, Pellagatti A, Cattan H, et al. Gene expression profiling of CD34+ cells in patients with the 5q- syndrome. *Br J Haematol* 2007;139(4):578–89.
58. Jimenez-Vacas JM, Herrero-Aguayo V, Montero-Hidalgo AJ, et al. Dysregulation of the splicing machinery is directly associated to aggressiveness of prostate cancer. *EBioMedicine* 2020;51:102547.
59. Verma S, Shankar E, Kalayci FNC, et al. Androgen Deprivation induces transcriptional reprogramming in prostate Cancer cells to develop stem cell-like characteristics. *Int J Mol Sci* 2020;21(24):9568.
60. Zhang L, Jiao M, Li L, et al. Tumorspheres derived from prostate cancer cells possess chemoresistant and cancer stem cell properties. *J Cancer Res Clin Oncol* 2012;138(4):675–86.
61. Ge Y, Schuster MB, Pundhir S, et al. The splicing factor RBM25 controls MYC activity in acute myeloid leukemia. *Nat Commun* 2019;10(1):172.
62. Rose AE, Satagopan JM, Oddoux C, et al. Copy number and gene expression differences between African American and Caucasian American prostate cancer. *J Transl Med* 2010;8:70.
63. Powell JJ. Epidemiology and pathophysiology of prostate cancer in African-American men. *J Urol* 2007;177(2):444–9.
64. Reddy S, Shapiro M, Morton Jr R, Brawley OW. Prostate cancer in black and white Americans. *Cancer Metastasis Rev* 2003;22(1):83–6.
65. Ka HI, Lee S, Han S, et al. Deubiquitinase USP47-stabilized splicing factor IK regulates the splicing of ATM pre-mRNA. *Cell Death Discov* 2020;6:34.
66. Das T, Park JK, Park J, et al. USP15 regulates dynamic protein-protein interactions of the spliceosome through deubiquitination of PRP31. *Nucleic Acids Res* 2017;45(8):4866–80.
67. Song EJ, Werner SL, Neubauer J, et al. The Prp19 complex and the Usp4Sart3 deubiquitinating enzyme control reversible ubiquitination at the spliceosome. *Genes Dev* 2010;24(13):1434–47.
68. Janowicz A, Michalak M, Krebs J. Stress induced subcellular distribution of ALG-2, RBM22 and hSlu7. *Biochimica et biophysica acta* 2011;1813(5):1045–9.
69. Montaville P, Dai Y, Cheung CY, et al. Nuclear translocation of the calcium-binding protein ALG-2 induced by the RNA-binding protein RBM22. *Biochimica et biophysica acta* 2006;1763(11):1335–43.
70. Santamaria D, Barriere C, Cerqueira A, et al. Cdk1 is sufficient to drive the mammalian cell cycle. *Nature* 2007;448(7155):811–5.
71. Gavet O, Pines J. Progressive activation of CyclinB1-Cdk1 coordinates entry to mitosis. *Dev Cell* 2010;18(4):533–43.
72. Boddy JL, Fox SB, Han C, et al. The androgen receptor is significantly associated with vascular endothelial growth factor and hypoxia sensing via hypoxia-inducible factors HIF-1a, HIF-2a, and the prolyl hydroxylases in human prostate cancer. *Clin Cancer Res* 2005;11(21):7658–63.
73. Keith B, Johnson RS, Simon MC. HIF1alpha and HIF2alpha: sibling rivalry in hypoxic tumour growth and progression. *Nat Rev Cancer* 2011;12(1):9–22.
74. Cimprich KA, Cortez D. ATR: an essential regulator of genome integrity. *Nat Rev Mol Cell Biol* 2008;9(8):616–27.
75. Johnson N, Cai D, Kennedy RD, et al. Cdk1 participates in BRCA1-dependent S phase checkpoint control in response to DNA damage. *Mol Cell* 2009;35(3):327–39.
76. Johnson N, Li YC, Walton ZE, et al. Compromised CDK1 activity sensitizes BRCA-proficient cancers to PARP inhibition. *Nat Med* 2011;17(7):875–82.
77. Yazinski SA, Comaills V, Buisson R, et al. ATR inhibition disrupts rewired homologous recombination and fork protection pathways in PARP inhibitor-resistant BRCA-deficient cancer cells. *Genes Dev* 2017;31(3):318–32.
78. Kim H, Xu H, George E, et al. Combining PARP with ATR inhibition overcomes PARP inhibitor and platinum resistance in ovarian cancer models. *Nat Commun* 2020;11(1):3726.
79. Neeb A, Herranz N, Arce-Gallego S, et al. Advanced prostate cancer with ATM loss: PARP and ATR inhibitors. *Eur Urol* 2021;79(2):200–11.
80. Murai J, Huang SY, Das BB, et al. Trapping of PARP1 and PARP2 by clinical PARP inhibitors. *Cancer Res* 2012;72(21):5588–99.
81. de Bono J, Mateo J, Fizazi K, et al. Olaparib for metastatic castration-resistant prostate cancer. *N Engl J Med* 2020;382(22):2091–102.